ACTA ABP BIOCHIMICA POLONICA

Vol. 70, No 4/2023
905–910
https://doi.org/10.18388/abp.2020_6806

Regular paper

miRNA-301 As a molecule promoting necrotizing enterocolitis by inducing inflammation

Dajun Zou, Fude Hu, Qili Zhou and Xiaoqing Xu

Department of Pediatric Surgery, Affiliated Hospital of Chengde Medical College, 36 Nanyingzi Street, Chengde, Hebei, 067000. P.R. China

Objective: Necrotizing enterocolitis (NEC) is a devastating inflammatory disease with high morbidity and mortality, mainly affecting premature infants. This study aimed to explore the role of miRNA-301a in the pathogenesis of NEC. Methods: The differentially expressed miRNAs and mRNAs were screened by collating RNA-Seq data from the GEO database of intestinal tissue samples. The differential miRNA-mRNAs regulatory network was constructed based on functional enrichment analysis. Newborn BALB/c mice were used to establish the NEC model. Haematoxylin and eosin staining was used to assess intestinal damage. The levels of IL-8 and TNF-α in mouse serum were evaluated by ELISA. qRT-PCR was used to detect the expression of miRNA-301a in intestinal tissues. Results: Bioinformatics analysis showed that miRNA-301a was involved in intestinal lesions. Intestinal tissue damage was reduced and serum levels of the inflammatory cytokines IL-8 and TNF-α were lower in NEC model mice treated with miRNA-301a antagonists. The level of miRNA-301a in intestinal tissues of NEC model mice was significantly higher than in the control group and miRNA-301a antagonists treated group. Conclusion: miRNA-301a plays an important role in the pathogenesis of NEC by promoting inflammation, and is a potential therapeutic target of NEC.

Keywords: necrotizing enterocolitis; miRNA-301a; bioinformatics analysis; inflammation

Received: 16 April, 2023; revised: 18 September, 2023; accepted: 19 October, 2023; available on-line: 28 November, 2023

e-mail: xiaoqingxu0419@163.com
Acknowledgements of Financial Support: This work was supported by the Hebei Medical Science Research Project (20210287).
Abbreviations: IBD, inflammatory bowel disease; NEC, necrotizing enterocolitis

INTRODUCTION

Despite decades of studies on necrotizing enterocolitis (NEC), NEC continues to be the most prevalent surgical condition that crises the lives of newborns (Meister *et al.,* 2020). Among very low birth weight infants, the prevalence of NEC ranges from 5% to 10%, and more than 50% of patients with NEC require surgery. Furthermore, the mortality rate of NEC treated by surgery ranges from 30% to 50% (Flahive *et al.,* 2020; Bell *et al.,* 2021). Hence, it is urgent to explore effective and reliable biomarkers for early identification of infants at risk of progression to improve the prognosis of NEC.

MicroRNAs (miRNAs) are a family of highly conserved RNAs, ranging in size from 19 to 24 nucleotides, and regulate the 3'-untranslated region of target mRNA transcripts (Chen *et al.,* 2013). In recent years, substantial progress has been achieved in understanding the role of diverse miRNAs in human diseases, including NEC (Cai *et al.,* 2022; Donda *et al.,* 2022). MiRNA-124 has been identified to facilitate NEC by targeting ROCK1 and promoting inflammatory cell infiltration in intestinal cells (Yin *et al.,* 2019). The increased expression of miRNA-141-3p could attenuate NEC damage to intestinal tissues by targeting MNX1 (Chen *et al.,* 2020). In addition, miRNA-301a facilitated intestinal mucosal inflammation by inducing IL-17A and TNF-α in inflammatory bowel disease (IBD) and colorectal cancer (He *et al.,* 2016). However, the role of miRNA-301a in NEC remains unclear.

In this study, a miRNA-mRNA regulatory network was successfully established by bioinformatics analysis and key miRNAs were screened based on this network. Next, a neonatal mouse NEC model was successfully established and the expression of miRNA-301a in the intestinal tissues and the levels of inflammatory factors TNF-α and IL-8 in the serum of mice were examined.

MATERIALS AND METHODS

Source of sample

MRNA and miRNA microarray data of intestinal tissue samples were gathered from GEO Datasets. GSE115513 includes 31 normal and 30 diseased intestinal tissue samples. GSE184093 includes 9 normal and 9 diseased intestinal tissue samples. The datasets were analysed by using PERL 5.30.2 (https://www.PERL.org/). The two datasets were sorted in the order of normal and experimental groups to acquire mRNA and miRNA data.

Differentially expressed miRNAs and mRNAs

The differentially expressed miRNAs and mRNAs were filtered by using the LIMMA package in the R software (https://rstudio.com/, version 3.6.2). The filtering criteria were set as |log2(fold change) |>1 and FDR (False Discovery Rate) <0.05. The "pheatmap" in R (3.6.2) was then applied to create differential volcano maps of the filtered differentially expressed mRNAs and miRNAs, respectively.

Identification of miRNA targets and construction of miRNA-mRNA regulatory network

The target genes of 222 differential miRNAs were predicted by using the gene function analysis tool FunRich (3.1.3) (http://www.funrich.org/). The differentially expressed mRNAs were crossed with the target genes of the miRNAs to generate the shared mRNAs and corresponding miRNAs, and the regulatory network was visualised using Cytoscape (3.7.2) (https://cytoscape.org/re-

lease_notes_3_7_2.html) to produce the miRNA-mRNA regulatory network.

GO and KEGG enrichment analyses

To further elucidate the biological functions of target genes in the regulatory network, GO (https://geneontology.org/docs/go-enrichment-analysis/) and KEGG enrichment analyses (https://www.genome.jp/kegg/pathway.html) of differential mRNAs were conducted with a screening condition of $p<0.05$ and $q<0.05$ and all outcomes were presented as bar graphs using the Bioconductor plugin in R software (Gao *et al.,* 2018).

Mice

Seventy-five newborn and pathogen-free BALB/c mice (7–10 days old) were obtained from the Animal Research Centre of Chengde Medical College (Chengde, China). All mice were housed at 28–30°C and 45–65% humidity for 12 hours on a light/dark cycle. This study was approved by the Animal Care and Use Committee of the Affiliated Hospital of Chengde Medical College (Approved No. 000134, date 2020-6-17). Mice were randomized into three groups (n=25 mice per group): the NEC group, the control group, and the NEC+anti-miRNA-301a group.

Neonatal mouse NEC model

The neonatal mouse NEC model was established as described previously (Nolan *et al.,* 2021). Mice in the NEC and NEC+anti-miRNA-301a groups (n=25) were fed Esbilac puppy formulae, which was complemented by bacteria cultured from the faeces of infants with severe NEC (12.5 µl of faecal slurry in 1 ml of formula). Briefly, a syringe filled with formulae was attached to a peripherally inserted central catheter (PICC) line. Next, the PICC line was gently introduced into the mouse's stomach by using forceps. Then the formulae were slowly dispensed into the stomach, and the PICC line was slowly withdrawn from the oral cavity (Nolan *et al.,* 2021). Mice were fed every 3 hours and after 3 feeds were placed under 5% O_2 + 95% N_2 for 10 minutes of stress to induce NEC. The feeding volume was 0.1 ml and gradually increased to 0.25 ml. The animals were sacrificed by decapitation on Day 5. For NEC+anti-miRNA-301a group, the mice were orally administered miRNA-301a antagonist (sequence mGmCmUmU-mUmGmAmCmAmAmUmAmCmUmAmUmUmGmC-mAmCmUmG, Genecreate LTD, Wuhan, China) following the manufacturer's manual once a day, starting at the beginning of NEC induction (Day 0) and continuing to Day 5.

Haematoxylin and eosin (H&E) staining

The intestinal tissues were dissected and washed with PBS at 4°C and fixed with 4% paraformaldehyde, paraffin-embedded, sectioned at 5 µm and stained with hematoxylin and eosin (H&E). The intestinal damage was analysed under a microscope with a 40x lens by two independent pathologists, who scored it double-blind according to published criteria (Zhang *et al.,* 2020).

MiRNA/mRNA isolation and reverse transcription

According to the manufacturer's instructions, TRIzol reagent (Invitrogen) was used to isolate total RNA from the intestinal tissues of the mice. Total RNA (2 µg) was used to generate cDNA by utilizing the Prime Script RT reagent kit (Takara, Tokyo, Japan).

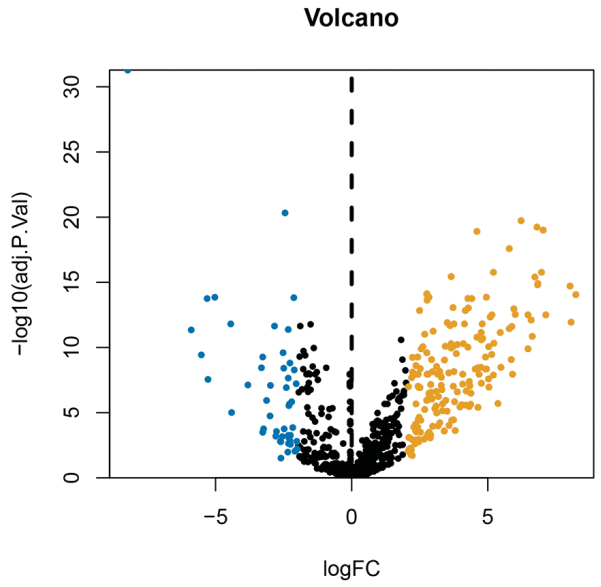

Figure 1. Volcanic map of differentially expressed miRNAs (orange represents upregulated miRNAs, blue represents downregulated miRNAs, and black represents miRNAs without a significant difference in expression).

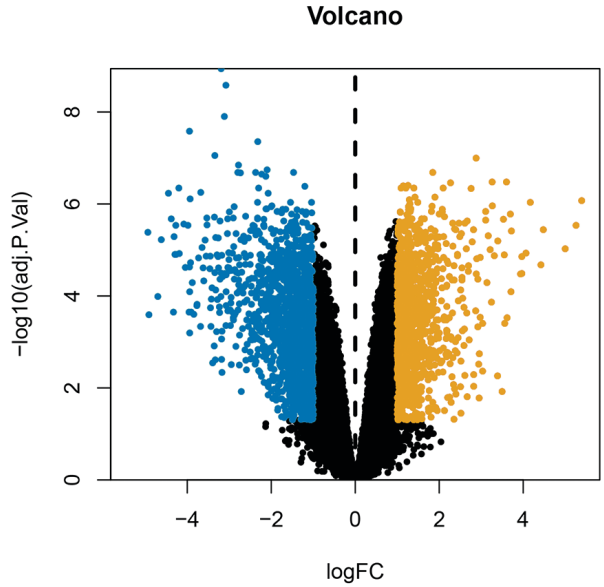

Figure 2. Volcanic map of differentially expressed mRNAs (orange represents upregulated mRNAs, blue represents downregulated mRNAs, and black represents miRNAs without a significant difference in expression).

qRT-PCR

QRT-PCR was undertaken by using SYBR Premix Ex Taq II (Perfect Real Time) (Takara, Tokyo, Japan). The gene-specific primers were purchased from Applied Biosystems (Foster City, CA, USA) with following sequences: U6: 5'-CTCGCTTCGGCAGCACA-3' and 5'-AACGCTTCACGAATTTGCGT-3', miRNA-301a: 5'-GGCAGTGCAATAGTATTGT-3' and 5'-TGGTGTCGTGGAGTCG-3'. U6 was used as an internal control for miR-301a expression. All experiments were in triplicates.

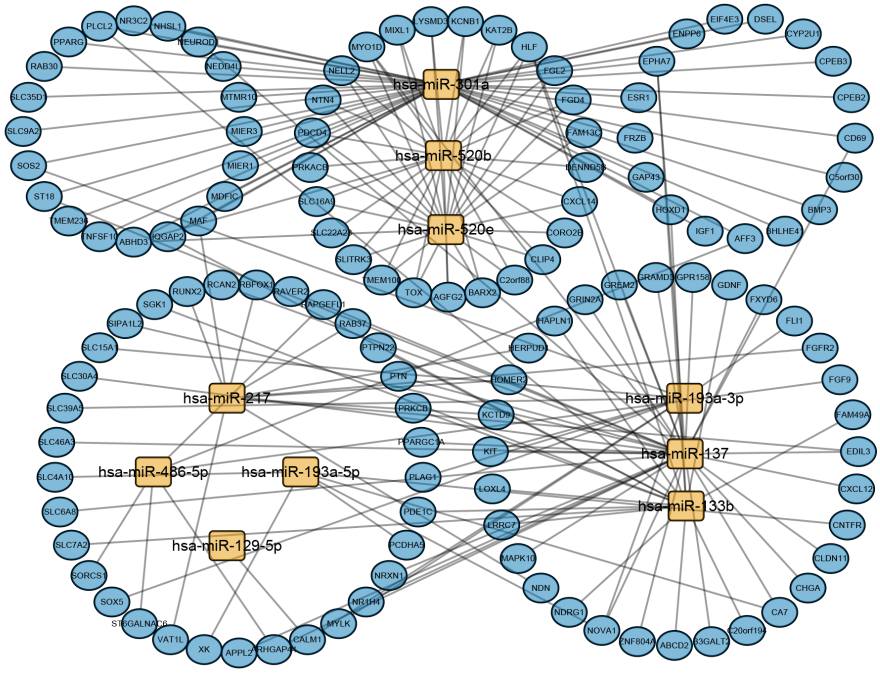

Figure 3. The miRNA-mRNA regulatory network (ellipses represent mRNAs, squares represent miRNAs, orange represents upregulated expression, blue represents downregulated expression, and connected lines represent targeted relationships).

ELISA

Serum was taken from all groups of mice. Paired ELISA kits for IL-8 and TNF-α (all from Enzyme Linked Biotechnology Co., Ltd., Shanghai, China) were used to evaluate the concentrations of IL-8 and TNF-α in the serum of the mice from each group. The optical density (OD) values of each well were recorded at 450 nm by a microplate reader.

Statistical analysis

Data were analysed by using SPSS 25.0 statistical software and expressed as mean ± standard deviation. The differences were considered to be statistically significant at $p<0.05$.

RESULTS

Differentially expressed miRNAs and mRNAs

After processing the dataset, a total of 222 differential miRNAs were screened, of which 172 miRNAs were highly expressed and 50 miRNAs were lowly expressed. Similarly, we obtained 2584 differential mRNAs, of which 1155 mRNAs were up-regulated and 1429 mR-

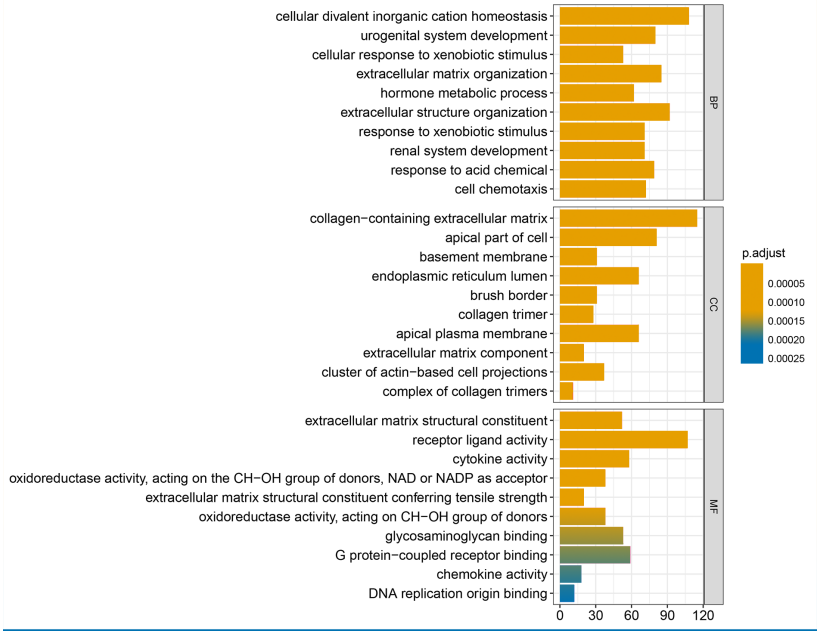

Figure 4. GO enrichment analysis of differentially expressed mRNAs.

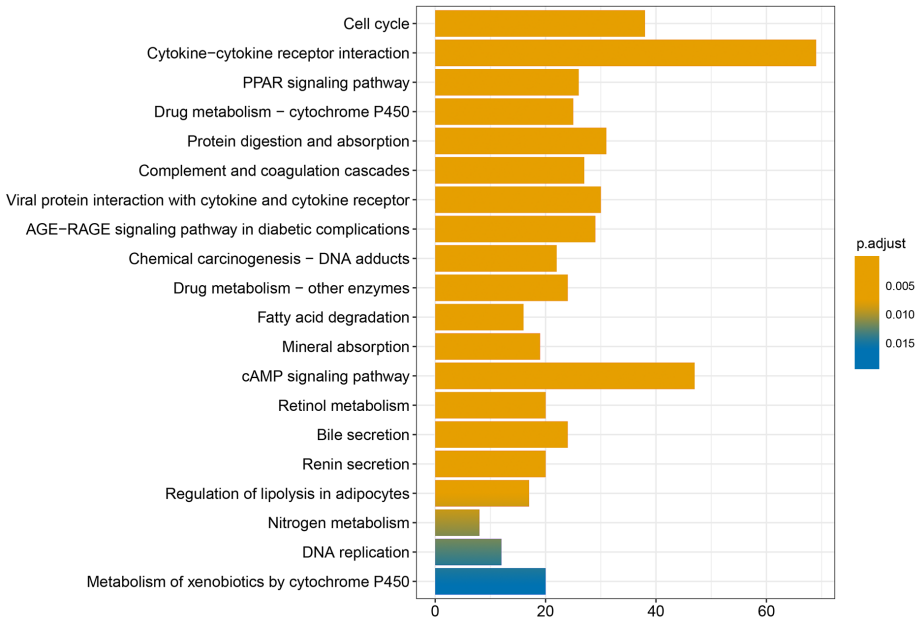

Figure 5. KEGG enrichment analysis of differentially expressed mRNAs.

NAs were down-regulated. The volcanoes of the differential miRNAs and mRNAs were subsequently mapped using R software (Figs 1 and 2).

Construction of miRNA-mRNA network and functional enrichment analysis

The FunRich (3.1.3) was used to predict the target genes of 222 differential miRNAs and a total of 2908 target genes were identified. The miRNA-mRNA regulatory network was then mapped using Cytoscape software (Fig. 3). The regulatory network showed that miRNA-301a regulated a greater number of mRNAs. We performed GO and KEGG enrichment analysis on 2584 different mRNAs using R language with $p<0.05$ and $q<0.05$ as screening conditions (Figs 4 and 5).

miRNA-301a antagonist reduced histological damage in NEC mice

We successfully established the NEC model using a previously published protocol (Nolan *et al.,* 2021) (Fig. 6A). During the experiments, two mice died both in the control and in NEC+anti-miRNA-301a groups, while three mice died in the NEC group. The difference in mortality among the three groups was not statistically significant ($p>0.05$). At the end of the experiments, the intestinal tissues of the mice in the NEC group showed a bluish-black colour compared to those of the mice in the control group. However, after treatment with the miRNA-301a antagonist, the degree of intestinal tissue necrosis in mice was significantly reduced (Fig. 6B).

The average histological score of the mice in the NEC group was 3.12±0.72, while the scores of the control

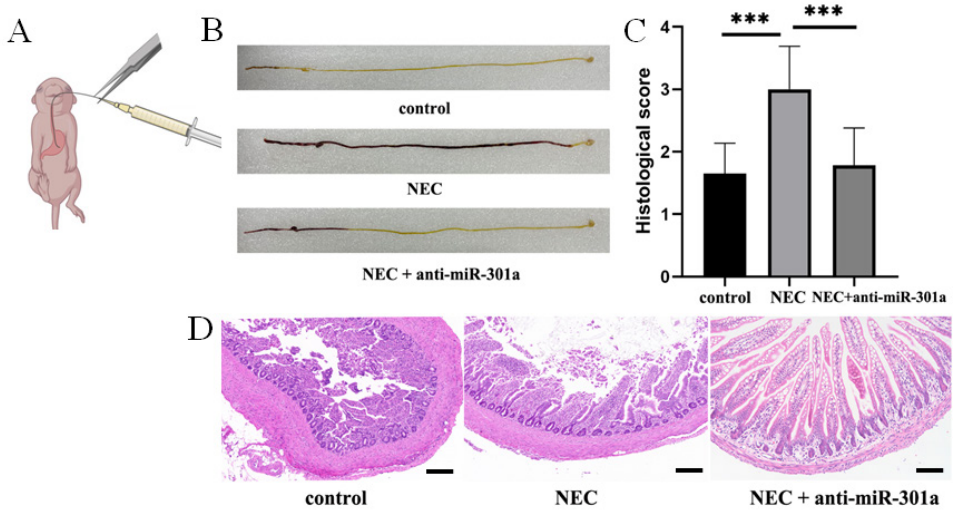

Figure 6. Inhibition of miRNA-301a ameliorated histological damage of NEC mice.
(**A**) Illustration of the delivery of NEC formulae to neonatal mice. (**B**) Representative gastrointestinal images of the different groups of mice. (**C**) H&E staining was used to evaluate the severity of tissue damage in different groups of mice (n=5) Mann-Whitney U-test. ***$p<0.001$. (**D**) Representative histological images of the terminal ileum in different groups of mice. Scale bar: 10 μm.

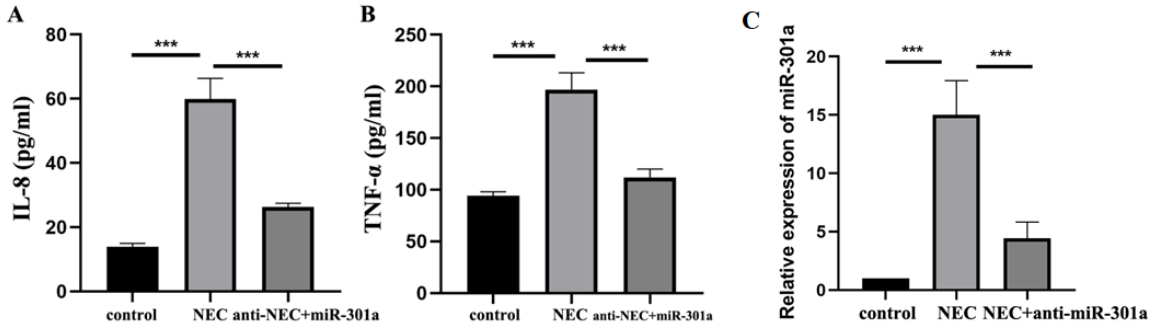

Figure 7. Inhibition of miRNA-301a reduced serum levels of inflammatory factors in NEC mice (n=5)
(**A**) Serum levels of IL-8 in different groups of mice. (**B**) Serum levels of TNF-α in different groups of mice. (**C**) Expression levels of miRNA-301a in intestinal tissues of different groups of mice. All experiments were in triplicates. ***$p<0.001$.

group were typically <2 points ($p<0.05$). After treatment with miRNA-301a antagonist, the average histological score was 1.78±0.60, and the inflammation grade was significantly reduced ($p<0.05$; Fig. 6C, D).

miRNA-301a antagonist reduced serum levels of IL-8 and TNF-α in NEC mice

The serum level of IL-8 was 13.95±1.05 pg/ml in the control group and 59.93±6.41 pg/ml in the NEC group ($p<0.05$). However, posttreatment with the miRNA-301a antagonist reduced IL-8 level to 26.23±1.22 pg/ml ($p<0.05$ compared to the NEC group; Fig. 7A).

Furthermore, the serum level of TNF-α was 94.16±3.92 and 197.04±16.19 in the control and NEC groups ($p<0.05$), respectively, and was 111.51±8.62 in mice that received miRNA-301a antagonist treatment ($p<0.05$ compared to the NEC group; Fig. 7B).

In addition, qRT-PCR showed that the expression level of miRNA-301a increased in the intestinal tissues of the NEC group ($p<0.05$ compared to the control group), but decreased in NEC mice treated with miRNA-301a antagonist ($p<0.05$ compared to the NEC group; Fig. 7C).

DISCUSSION

NEC is the main catastrophic cause of death in surviving premature infants. The pathogenesis of NEC as well as potential strategies for NEC prevention and treatment remain elusive, although it is evident that the inflammatory cascade plays an important role in the development of NEC (Niño *et al.,* 2016; Liu *et al.,* 2019). In this study, we successfully established an NEC mouse model to explore the role of miRNA-301a in the pathogenesis of NEC, and we proved the association between high expression of miRNA-301a and increased severity of NEC. In addition, our study revealed that high expression of miRNA-301a promoted the release of inflammatory factors IL-8 and TNF-α.

Numerous studies have proven that non-encoding RNAs regulate inflammation through a variety of pathways (Zhou *et al.,* 2021; Yang & Ge, 2018). miRNA-301a was highly expressed in peripheral blood mononuclear cells and inflamed mucosa of patients with active IBD and may promote TNF-α production by targeting SNIP1, ultimately facilitating the pathogenesis of IBD (He *et al.,* 2016). miRNA-301a also inhibited the expression of BTG1, thereby reducing the integrity of the epithelium, promoting inflammation of the mouse colon and stimulating tumorigenesis (He *et al.,* 2017). In this study we found that the pathological inflammation of the mouse intestinal tissue was reduced after we treated NEC mice with miRNA-301a antagonist, indicating that miRNA-301a plays an important role in the inflammatory progression of NEC.

For newborns with NEC, IL-8, IL-10, and TNF-α can be used as biomarkers for early diagnosis (Seliga-Siwecka & Kornacka, 2013). Combined analysis of IFN-γ-inducible protein 10 and TNF-α showed a specificity of 80% and a sensitivity of 90% (Weissenbacher *et al.,* 2013). In this study, we focused on TNF-α and IL-8, and found that the serum levels of inflammatory cytokines IL-8 and TNF-α were reduced after we treated NEC mice with miRNA-301a antagonist, suggesting that miRNA-301a may be a potential therapeutic target for NEC. In future studies, we need to examine other pro-inflammatory interleukins such as IL-1, IL-6 and IL-10 (Fu *et al.,* 2023).

Studies have shown that microRNAs play an important role in energy metabolism, immune regulation, homeostasis, cell apoptosis, cell proliferation and differentiation (Qi *et al.,* 2022; Zhong *et al.,* 2018; Zhang *et al.,* 2022; Liu *et al.,* 2022; Dai *et al.,* 2022; Chen *et al.,* 2021). Interference with these key cell functions can lead to an increase in apoptosis and inflammation and a decrease in repair capacity, which may be crucial in the pathogenesis of NEC (Premkumar *et al.,* 2014; Ng *et al.,* 2015). To further explore the potential mechanism of miRNA-301a in promoting NEC, we need to identify target genes of miRNA-301a that medicate the effects of miRNA-301a on cell proliferation, apoptosis, inflammation, mentalism and autophagy involved in the progression of NEC.

In conclusion, although further studies are necessary to confirm the role of miRNA-301a in MEC, our results provide the first evidence that miRNA-301a plays an important role in the pathogenesis of NEC by promoting inflammation, and is a potential therapeutic target of NEC.

Declarations

Availability of data and material. All data and materials are included in this manuscript.

Competing interests. The authors have no conflict of interest.

Authors' contributions. XX designed and supervised the study. DZ, FH and QZ performed the experiments and analyzed the data. All authors read and approved the final manuscript.

REFERENCES

Bell RL, Withers GS, Kuypers FA, Stehr W, Bhargava A (2021) Stress and corticotropin releasing factor (CRF) promote necrotizing enterocolitis in a formula-fed neonatal rat model. *PLoS One* **16**: e0246412. https://doi.org/10.1371/journal.pone.0246412

Cai L, Lai D, Gao J, Wu H, Shi B, Ji H, Tou J (2022) The role and mechanisms of miRNAs in neonatal necrotizing enterocolitis. *Front Pediatrician* **10**: 1053965. https://doi.org/10.3389/fped.2022.1053965

Chen CZ, Schaffert S, Fragoso R, Loh C (2013) Regulation of immune responses and tolerance: the microRNA perspective. *Immunol Rev* **253**: 112–128. https://doi.org/10.1111/imr.12060

Chen H, Zeng L, Zheng W, Li X, Lin B (2020) Increased expression of microRNA-141-3p improves necrotizing enterocolitis of neonates through targeting MNX1. *Front Pediatr* **8**: 385. https://doi.org/10.3389/fped.2020.00385

Chen X, Zhang H, Li L, Chen W, Bao T, Li B (2021) miR-5100 mediates migration and invasion of melanomatous cells *in vitro via* targeting SPINK5. *J Comp Mol Sci Genet* **1**: 14–23. Retrieved from https://mbgm.journals.publicknowledgeproject.org/index.php/mbgm/article/view/1395

Dai D, Li B, Su Y, Li L, Fang X, Chen Y, Wang Y, Xu W (2022) Aminophylline inhibits the expression of inflammatory factors in airway smooth muscle cells under hypoxia through miR-138-5p/HIF1A axis. *J Comp Mol Sci Genet* **1**: 15–20. Retrieved from https://mbgm.journals.publicknowledgeproject.org/index.php/mbgm/article/view/2240

Donda K, Bose T, Dame C, Maheshwari A (2022) The impact of microRNAs in neonatal necrotizing enterocolitis and other inflammatory conditions of intestine: a review. *Curr Pediatr Rev* **19**: 5–14. https://doi.org/10.2174/1573396318666220117102119

Flahive C, Schlegel A, Mezoff EA (2020) Necrotizing enterocolitis: updates on morbidity and mortality outcomes. *J Pediatr* **220**: 7–9. https://doi.org/10.1016/j.jpeds.2019.12.035

Fu J, Chen R, Zhang Z, Zhao J, Xia T (2023) An inflammatory-related genes signature based model for prognosis prediction in breast cancer. *Oncol Res* **31**: 157–167. https://doi.org/10.32604/or.2023.027972

Gao X, Chen Y, Chen M, Wang S, Wen X, Zhang S (2018) Identification of key candidate genes and biological pathways in bladder cancer. *PeerJ* **6**: e6036. https://doi.org/10.7717/peerj.6036

He C, Shi Y, Wu R, Sun M, Fang L, Wu W, Liu C, Tang M, Li Z, Wang P, Cong Y, Liu Z (2016) miR-301a promotes intestinal mucosal inflammation through induction of IL-17A and TNF-α in IBD. *Gut* **65**: 1938–1950. https://doi.org/10.1136/gutjnl-2015-309389

He C, Yu T, Shi Y, Ma C, Yang W, Fang L, Sun M, Wu W, Xiao F, Guo F, Chen M, Yang H, Qian J, Cong Y, Liu Z (2017) MicroRNA 301A Promotes intestinal inflammation and colitis-associated cancer development by inhibiting BTG1. *Gastroenterology* **152**: 1434–1448. e15. https://doi.org/10.1053/j.gastro.2017.01.049

Liu J, Li Y, Feng Y, Pan L, Xie Z, Yan Z, Zhang L, Li M, Zhao J, Sun J, Hong L (2019) Patterned progression of gut microbiota associated with necrotizing enterocolitis and late onset sepsis in preterm infants: a prospective study in a Chinese neonatal intensive care unit. *PeerJ* **7**: e7310. https://doi.org/10.7717/peerj.7310

Liu Y, Wang M, Deng T, Liu R, Ning T, Bai M, Ying G, Zhang H, Ba Y (2022) Exosomal miR-155 from gastric cancer induces cancer-associated cachexia by suppressing adipogenesis and promoting brown adipose differentiation *via* C/EPBβ. *Cancer Bio Med* **19**: 1301–1314. https://doi.org/10.20892/j.issn.2095-3941.2021.0220

Meister AL, Doheny KK, Travagli RA (2020) Necrotizing enterocolitis: It's not all in the gut. *Exp Biol Med (Maywood)* **245**: 85–95. https://doi.org/10.1177/1535370219891971

Ng PC, Chan KY, Leung KT, Tam YH, Ma TP, Lam HS, Cheung HM, Lee KH, To KF, Li K (2015) Comparative MiRNA expressional profiles and molecular networks in human small bowel tissues of necrotizing enterocolitis and spontaneous intestinal perforation. *PLoS One* **10**: e0135737. https://doi.org/10.1371/journal.pone.0135737

Niño DF, Sodhi CP, Hackam DJ (2016) Necrotizing enterocolitis: new insights into pathogenesis and mechanisms. *Nat Rev Gastroenterol Hepatol* **13**: 590–600. https://doi.org/10.1038/nrgastro.2016.119

Nolan LS, Gong Q, Hofmeister HN, Good M (2021) A protocol for the induction of experimental necrotizing enterocolitis in neonatal mice. *STAR Protoc* **2**: 100951. https://doi.org/10.1016/j.xpro.2021.100951

Premkumar MH, Sule G, Nagamani SC, Chakkalakal S, Nordin A, Jain M, Ruan MZ, Bertin T, Dawson B, Zhang J, Schady D, Bryan NS, Campeau PM, Erez A, Lee B (2014) Argininosuccinate lyase in enterocytes protects from development of necrotizing enterocolitis. *Am J Physiol Gastrointest Liver Physiol* **307**: G347–G354. https://doi.org/10.1152/ajpgi.00403.2013

Qi L, Xu X, Li B, Chang B, Wang S, Liu C, Wu L, Zhou X, Wang Q (2022) Dihydroartemisinin ameliorates palmitate-induced apoptosis in cardiomyocytes *via* regulation on the miR-133b/Sirt1 axis. *Biocell* **46**: 989–998. https://doi.org/10.32604/biocell.2022.018014

Seliga-Siwecka JP, Kornacka MK (2013) Neonatal outcome of preterm infants born to mothers with abnormal genital tract colonisation and chorioamnionitis: a cohort study. *Early Hum Dev* **89**: 271–275. https://doi.org/10.1016/j.earlhumdev.2012.10.003

Weissenbacher T, Laubender RP, Witkin SS, Gingelmaier A, Schiessl B, Kainer F, Friese K, Jeschke U, Dian D, Karl K (2013) Diagnostic biomarkers of pro-inflammatory immune-mediated preterm birth. *Arch Gynecol Obstet* **287**: 673–685. https://doi.org/10.1007/s00404-012-2629-3

Yang T, Ge B (2018) miRNAs in immune responses to *Mycobacterium tuberculosis* infection. *Cancer Lett* **431**: 22–30. https://doi.org/10.1016/j.canlet.2018.05.028

Yin Y, Qin Z, Xu X, Liu X, Zou H, Wu X, Cao J (2019) Inhibition of miR-124 improves neonatal necrotizing enterocolitis *via* an MYPT1 and TLR9 signal regulation mechanism. *J Cell Physiol* **234**: 10218–10224. https://doi.org/10.1002/jcp.27691

Zhang J, Wang C, Guo Z, Da B, Zhu W, Li Q (2021) miR-223 improves intestinal inflammation through inhibiting the IL-6/STAT3 signaling pathway in dextran sodium sulfate-induced experimental colitis. *Immun Inflamm Dis* **9**: 319–327. https://doi.org/10.1002/iid3.395

Zhang T, Wang J, Wang D, Xu K, Wu L, Wang X, Wang W, Deng L, Liang J, Lv J, Hui Z, Zhou Z, Feng Q, Xiao Z, Chen D, Wang J, Wang L, Bi N (2022) The time-series behavior of systemic inflammation-immune status in predicting survival of locally advanced non-small cell lung cancer treated with chemoradiotherapy. *J Natl Cancer Center* **2**: 33–40. https://doi.org/10.1016/j.jncc.2021.11.003

Zhong L, Simard MJ, Huot J (2018) Endothelial microRNAs regulating the NF-κB pathway and cell adhesion molecules during inflammation. *FASEB J* **32**: 4070–4084. https://doi.org/10.1096/fj.201701536R

Zhou J, Ji X, Wang Y, Wang X, Mao Y, Yang Z (2021) Long intergenic noncoding RNAs differentially expressed in *Staphylococcus aureus*-induced inflammation in bovine mammary epithelial cells. *Biocell* **45**: 1033–1044. https://doi.org/10.32604/biocell.2021.015586